photochem

MDPI

Article

Ar-Matrix Studies of the Photochemical Reaction between CS_2 and ClF: Prereactive Complexes and Bond Isomerism of the Photoproducts

Michelle T. Custodio Castro [1], Carlos O. Della Védova [1], Helge Willner [2] and Rosana M. Romano [1,*]

[1] CEQUINOR (UNLP, CCT-CONICET La Plata, Associated with CIC), Departamento de Química, Facultad de Ciencias Exactas, Universidad Nacional de La Plata, Blvd. 120 N° 1465, La Plata 1900, Argentina
[2] Anorganische Chemie, Bergische Universität Wuppertal, Gaußstraße 20, D-42097 Wuppertal, Germany
* Correspondence: romano@quimica.unlp.edu.ar

Abstract: In this work, prereactive complexes, reaction products, and conformational preferences derived from the photochemical reaction between CS_2 and ClF were analyzed following the codeposition of the reactants trapped in argon matrices at cryogenic temperatures. After codeposition of CS_2 and ClF diluted in Ar, the formation of van der Waals complexes is observed. When the mixture is subsequently irradiated by means of broad-band UV-visible light ($225 \leq \lambda \leq 800$ nm), fluorothiocarbonylsulfenyl chloride (FC(S)SCl) and chlorothiocarbonylsulfenyl fluoride (ClC(S)SF) are produced. These species exist as two stable planar anti- and syn-conformers (anti- and syn- of the C=S double bond with respect to the S–Cl or S–F single bond, respectively). For both novel molecules, anti-FC(S)SCl and anti-ClC(S)SF are the lowest-energy computed rotamers. As expected due to the photochemical activity of these species, additional reaction products due to alternative or subsequent photochannels are formed during this process.

Keywords: matrix-isolation; photochemistry; carbon disulfide; chloromonofluoride

Citation: Custodio Castro, M.T.; Della Védova, C.O.; Willner, H.; Romano, R.M. Ar-Matrix Studies of the Photochemical Reaction between CS_2 and ClF: Prereactive Complexes and Bond Isomerism of the Photoproducts. *Photochem* **2022**, *2*, 765–778. https://doi.org/10.3390/photochem2030049

Academic Editors: Gulce Ogruc Ildiz and Licinia L.G. Justino

Received: 19 July 2022
Accepted: 31 August 2022
Published: 2 September 2022

1. Introduction

The preparation and study of properties of new covalent compounds has been and will be a central challenge for chemists of all time. Through this knowledge, chemists and scientists from related branches can design their work with novelty and unconventionality. In this context, the synthesis of small and new covalent compounds, as a linking piece between disciplines such as inorganic and organic chemistry, biology, biochemistry, medicine, physics, materials science, different spectroscopies, and photochemistry, is one of the goals of the present work. An emerging edge to be approached with the systematized information obtained is the one referring to the world of conformations and their equilibria.

The matrix-isolation technique in combination with photochemistry is particularly suitable for the isolation of novel small molecules for which no other alternative synthetic route was found, and also the understanding of the reaction pathways that may lead to more efficient control of the reactions [1–3]. Our research group has been able to isolate and study different families of novel molecules by matrix-isolation photochemistry coupled with FTIR spectroscopy (see, for example, Refs. [4–7] and references cited therein). A prerequisite for a photochemical reaction in matrix conditions to occur is that the reactants are held in the same matrix site. Due to the isolation conditions, the reaction is favored when a prereactive molecular complex is formed between the reactants. Furthermore, the geometry of the prereactive complex often determines the course of the photochemical reaction [7].

In this work, we explored the Ar-matrix photochemical reaction between carbon disulfide and chlorine monofluoride. The codeposition of CS_2 with ClF, both diluted in Ar, gives rise to the formation of van der Waals complexes, which are stable species from

a thermodynamic point of view. Several molecular complexes between ClF and different Lewis bases were previously studied by a combination of matrix-isolation technique with IR spectroscopy [6,8–16]. A T-shaped structure for 1:1 complexes of ClF with a series of alkynes and alkenes was inferred from the Ar-matrix IR spectra, with the interhalogen molecule interacting with the π electron density of the alkyne or alkene [8]. It was reported that complexes with alkenes produced larger shifts than complexes formed with alkynes, and the wavenumber shifts increased with increasing methyl substitution near the carbon-carbon multiple bond. A redshift of the ClF stretching vibrational mode was also observed for 1:1 molecular complexes of H_2Se and H_3As with the interhalogen molecule isolated in solid Ar, interpreted as an electron density transfer from the Se or As atom to the lowest unoccupied antibonding molecular orbital of ClF [9]. Since the base subunit is donating nonbonding electron density, only slight perturbations were observed in the base modes of the complex. Comparable results were obtained for complexes of ClF with sulfur and nitrogen-containing macrocycles [11].

After irradiation, the formation of the novel FC(S)SCl and ClC(S)SF species were detected by FTIR spectra of the matrices. The relative stabilities of the syn- and anti-rotamers of each of these molecules are discussed, and compared with analogue molecules. Their formation could be related to roaming mechanisms or frustrated dissociation occurring during the photoisomerization process of these penta-atomic species. The identification of the van der Waals complexes and the two conformers of both novel molecules, FC(S)SCl and ClC(S)SF, were assisted by the predictions of DFT calculations.

2. Materials and Methods

CAUTION: Handling pure fluorine implies that pertinent precautions should be observed. The reactor and the vacuum lines have to be adequately pretreated with fluorine prior to use. ClF was obtained by the reaction of stoichiometric amounts of F_2 (Solvay, Germany) and Cl_2 at 250 °C in a Monel vessel. The reaction mixture was subsequently distilled to separate ClF from Cl_2, ClF_3 and F_2. The interhalogen ClF was transferred into a 1 L stainless-steel container at a vacuum line and diluted with Ar in a ClF:Ar = 2:100 proportion. Separately, a sample of CS_2 was mixed with argon in a 0.5 L glass container in 1:100 ratio. Both containers were connected via needle valves and stainless-steel capillaries to the spray-on nozzle of the matrix support. About 0.5–1.0 mmol of the gas mixtures were codeposited within 10–20 min on the mirror support at 15 K (a mirror plane of a rhodium-plated copper block). A 150 W high-pressure Xe lamp (Heraeus, Hanau, Germany) in combination with a 225 nm cut-off filter were used for the matrix irradiation. The light was directed through water-cooled quartz lenses onto the matrix for 1 to a maximum of 90 min. The photolysis process was followed by IR spectroscopy. Details of the matrix apparatus are given elsewhere [17]. Matrix IR spectra were recorded on a Bruker IFS 66v/S spectrometer with a resolution of 0.5 cm^{-1} in absorption/reflection mode. The IR spectra were processed by curve-fitting analysis using the OPUS Program and the intensities were determined integrating the areas of the individual peaks.

Quantum chemical calculations were performed using either Gaussian 03 [18] or Gaussian 09 [19] program. Density Functional Theory (B3LYP and B3LYP-D3) method was tried in combination with the 6-311+G(d,p) basis sets. Relaxed two-dimensional scans for the 1:1 CS_2:ClF complexes were performed in order to find the energy minima. Geometry optimizations were sought using standard gradient techniques by simultaneous relaxation of all the geometrical parameters. The calculated vibrational properties correspond in all cases to potential energy minima with no imaginary frequencies.

The binding energies of the molecular complexes were calculated using the correction proposed by Nagy et al. [20]. The basis set superposition errors (BSSE) have been calculated by applying the counterpoise procedure developed by Boys and Bernardi [21]. The electronic transitions for the previously optimized structure of the molecular complexes were calculated using the TD-DFT formalisms, with a maximum of 100 states and S = 1 [22,23].

3. Results and Discussion

3.1. Codeposition of CS_2 + ClF in Ar Matrix

The reactants were codeposited simultaneously in the mirror plane cooled to about 15 K. The FTIR spectra of the matrix obtained before irradiation were analyzed and compared with the experimental spectra of the monomers taken in similar conditions. The signal corresponding to the CS_2 antisymmetric vibration, $\nu_{as}CS_2$, of the carbon disulfide molecule appears in the spectrum at 1527.9 cm^{-1} (Figure 1). In addition, there are also absorptions at 1524.4 cm^{-1} assigned to the ^{34}SCS isotopologue and at 1533.5 cm^{-1} originating by the dimer $(CS_2)_2$. This dimer was also formed in the reaction between CS_2 and F_2 achieved under similar conditions to the present work, where the corresponding band appears at 1533.6 cm^{-1} [4]. Figure 1 also shows a band at 2169.5 cm^{-1}, assigned to a combination mode of CS_2 ($\nu_{as}CS_2$ + ν_sCS_2). The ClF interhalogen presents FTIR signals at 767.0 and 759.8 cm^{-1}, due to $\nu^{35}ClF$ and $\nu^{37}ClF$ vibrations, and also mirror bands of lower intensity at 769.9 and 762.7 cm^{-1}, attributed to matrix effects, and at 755.5 and 748.7 cm^{-1} due to molecular aggregation (Figure 2) [6].

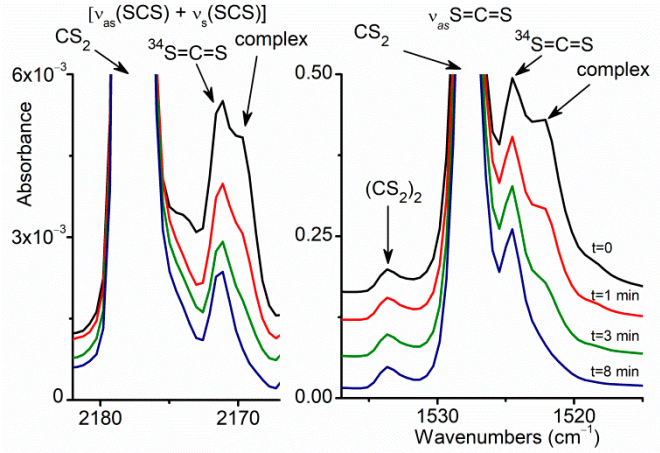

Figure 1. FTIR spectra of the CS_2/ClF/Ar matrix (CS_2:ClF:Ar = 1:2:200) at about 15 K after deposition (**top**, black trace) and, from **top** to **bottom**, after 1 (red trace), 3 (green trace) and 8 min (blue trace) of irradiation with broad-band UV-visible light ($225 \leq \lambda \leq 800$ nm) in the 2182–2167 and 1537–1515 cm^{-1} regions.

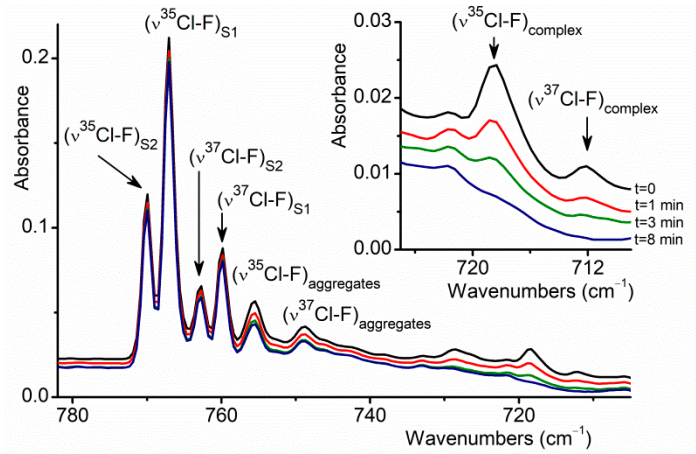

Figure 2. FTIR spectra of the CS_2/ClF/Ar matrix (CS_2:ClF:Ar = 1:2:200) at about 15 K after deposition (**top**, black trace) and, from **top** to **bottom**, after 1 (red trace), 3 (green trace) and 8 min (blue trace) of irradiation with broad-band UV-visible light ($225 \leq \lambda \leq 800$ nm) in the 782–705 cm^{-1} region.

At this stage of the experiment, that is, when the matrix was not yet irradiated, four new bands were observed at 2169.5, 1522.2, 718.5 and 712.2 cm^{-1} (see Figures 1 and 2).

These bands are not present in the experimental spectrum of the isolated monomers of CS_2 and ClF and their subsequent behavior during the photochemical irradiation of the matrix; that is, the tendency to decrease their intensities with the irradiation time allows for them to be assigned to signals originated by the formation of van der Waals complexes between CS_2 and ClF. In order to dispose of photochemical kinetic data that allow for relevant information to be provided to the present study, the matrix formed with a 1:2:200 CS_2:ClF:Ar concentration was irradiated in the UV-visible range ($\lambda > 225$ nm) for 1, 3, 8, 15, 45, and 90 min. As can be observed in Figures 1 and 2, these new absorptions completely vanish after 8 min of irradiation. Figure 3 shows the variation of the FTIR band intensities assigned to the monomers, CS_2 and ClF, and that to the CS_2:ClF van der Waals complex as a function of the irradiation time. As can be observed in Figure 3, while the intensities of the IR bands of the monomers show a slight decrease (their intensities after 45 min of irradiation are approximately 80% of the initial values), the IR features assigned to the complex follow a different kinetic behavior, disappearing after 8 min of exposition to broad-band radiation. Figure 3 also reveals that the absorptions attributed to the complex follow the same pattern as a function of irradiation time, a necessary condition to be assigned to the same species.

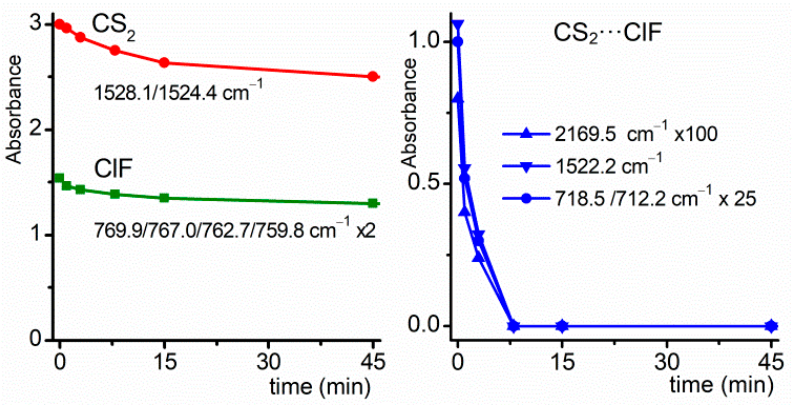

Figure 3. Plots of the intensities of the bands in the FTIR spectra of the CS_2/ClF/Ar matrix (CS_2:ClF:Ar = 1:2:200) at about 15 K vs irradiation times with broad-band UV-visible light ($225 \leq \lambda \leq 800$ nm). **Left**: bands assigned to CS_2 and ClF; **Right**: bands assigned to the 1:1 CS_2:ClF van der Walls complex.

Computational calculations are especially valuable for reproducing experimental results. The geometry of the stable systems formed by CS_2 and ClF were determined searching for the energy minima of the complexes varying the S···Cl and S···F distances in 0.1 Å steps and the C=S···Cl and C=S···F intermolecular angles in 10° steps. Figure 4 shows the contour map of the potential energy surface for the CS_2···ClF complex calculated with the B3LYP/6-311G+(d,p) approximation. On the right part of Figure 4, the molecular model corresponding to the optimized structure of the energy minimum calculated with the same theoretical approximation is also represented in Figure 4. Equivalently, Figure 5 shows the molecular complex that links the CS_2 molecule with the fluorine atom of the ClF interhalogen. As in many branches of chemistry, fluorine again shows its particularity. When the van der Waals complex is formed using it as a bridge, the geometry of the complex is now linear.

The calculated geometrical parameters of the optimized structures of the two complexes are presented as Supporting Information (Table S1). An intermolecular distance S···Cl of 2.9411 Å, which corresponds to a van der Waals penetration distance of 0.62 Å, and an intermolecular C=S···Cl angle of 97.9° are predicted for the CS_2···ClF complex. On the other hand, for the CS_2···FCl structure, a value of 3.2531 Å is obtained for the S···F distance, that gives a 0.05 Å van der Waals penetration distance. The predicted intermolecular C=S···F angle for the optimized structure is 180.0°, as shown in Figure 5. According to the B3LYP/6-311G+(d,p) approximation, the CS_2···FCl complex is 1.83 kcal/mol (7.66 kJ/mol) higher

in energy than the $CS_2\cdots ClF$ form. The former structure presents almost the same energy that the isolated monomers ($\Delta E = E(CS_2\cdots FCl)–E(CS_2)–E(FCl) = -0.06$ kcal/mol), while the latter complex is predicted to be energetically favored with respect to the monomers by 1.89 kcal/mol. The Supporting Information contains detailed data of the calculated energies and the corresponding corrections (Table S2). In agreement with this stability difference, a value of −9.79 and −0.71 kcal/mol were obtained for the most important contribution to the orbital stabilization energies of the $CS_2\cdots ClF$ and $CS_2\cdots FCl$ complexes, respectively. The charge transfer resulting in the complex formation occurring mainly from the free-electron pair of the sulfur atom to the σ antibonding orbital of the ClF molecule ($lpS\rightarrow\sigma^*_{ClF}$) acquires a value of −0.0894 e for the $CS_2\cdots ClF$ complex. On the other hand, for the $CS_2\cdots FCl$ structure, a much lower charge transfer of −0.0013 e was predicted, while the main orbital interactions occur from the ClF unit to the CS_2 molecule: σClF→RyS (−0.71 kcal/mol) and lpF→σ*C=S (−0.29 kcal/mol). Figure 6 shows a schematic representation of these two orbital interactions. The geometries of the complexes are consistent with the main contributions to the orbital interactions in each case. In the $CS_2\cdots ClF$ adduct, carbon disulfide acts as a donor molecule and chlorine monofluoride as the acceptor unit, favoring the angular geometry. The donor and acceptor roles are inverted in the $CS_2\cdots FCl$ complex, determining the collinear geometry.

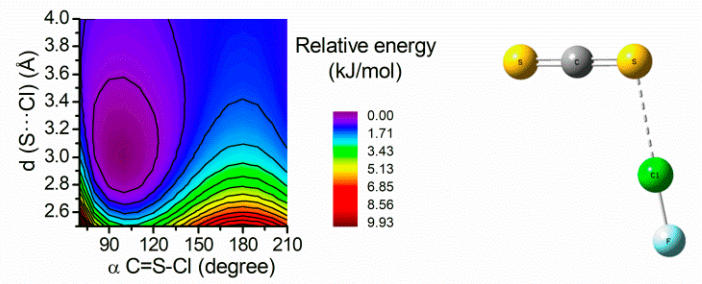

Figure 4. Contour map of the potential energy surface of the S=C=S···ClF molecular complex calculated by the variation of the S···Cl intermolecular distance from 2.5 to 4.0 Å in 0.1 Å steps and the C=S···Cl intermolecular angle from 70 to 210° in 10° steps with the B3LYP/6-311G+(d,p) (**left**) and molecular model of the optimized minimum (**right**).

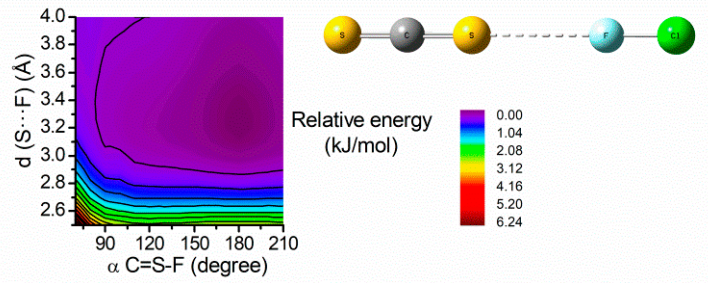

Figure 5. Contour map of the potential energy surface of the S=C=S···FCl molecular complex calculated by the variation of the S···Cl intermolecular distance from 2.5 to 4.0 Å in 0.1 Å steps and the C=S···F intermolecular angle from 70 to 210° in 10° steps with the B3LYP/6-311G+(d,p) (**left**) and molecular model of the optimized minimum (**right**).

The vibrational spectra of the complexes were also calculated using the B3LYP/6-311G+(d,p) approximation, and the predicted wavenumbers shifts with respect to the monomers were compared with the experimental findings. A complete list of the calculated frequencies is presented as Supporting Information in Table S3, while Table 1 compiles the vibrational wavenumbers that were observed in the experimental FTIR spectra.

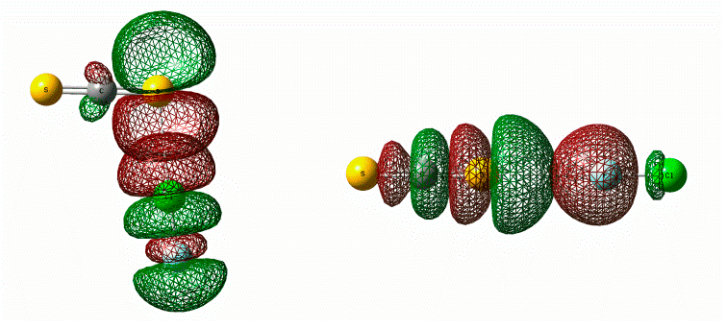

Figure 6. Schematic representations of the main contributions to the orbital interactions in the $CS_2\cdots ClF$ (**left**) and $CS_2\cdots FCl$ (**right**) complexes calculated with the B3LYP/6-311G+(d,p).

Table 1. Selected wavenumbers for the different complexes formed between CS_2 and ClF computed with the B3LYP/6-311+G(d,p) approximation (wavenumbers are in cm^{-1} and relative IR intensities are given between parentheses) and comparison with the experimental value.

Ar Matrix		B3LYP/6-311+G(d,p)				Tentative Assignment
		S=C=S···Cl−F		S=C=S···F−Cl		
ν (cm^{-1})	Δν (cm^{-1}) [a]	ν (cm^{-1}) [b]	Δν (cm^{-1}) [a]	ν (cm^{-1}) [b]	Δν (cm^{-1}) [a]	
2169.5	−8.3					ν_{as}(SCS) + ν_s(SCS)
1522.2	−5.7	1547.1 (100)	−6.2	1552.2 (100)	−1.9	ν_{as}(SCS)
		671.8 (<1)	−2.1	673.3 (<1)	−0.6	ν_s(SCS)
718.5	−48.6	646.5 (31.8)	−93.3	740.3 (3.8)	+0.7	ν(^{35}Cl–F)
712.2	−47.7	640.8 (10.2)	−92.2	733.2 (1.2)	+0.5	ν(^{37}Cl–F)

[a] $\Delta\nu = \nu_{complex} - \nu_{monomer}$. [b] Relative intensities between parentheses.

The simulated IR spectrum of the $CS_2\cdots ClF$ complex is the one that best reproduces the experimental results. The calculated ν_{as}(S=C=S) is shifted by −6 cm^{-1}, in complete agreement with the experimental value (see Figure 1). The direction of the shift in the Cl–F stretching vibrational mode is what allows the structure to be assigned with confidence. Meanwhile, in the complex that interacts through the Cl atom of the diatomic molecule, a shift towards lower wavenumbers of approximately 90 cm^{-1} is predicted, in accordance with the redshift observed in the FTIR spectra depicted in Figure 2; for the $CS_2\cdots FCl$ adduct, the shift is less than 1 cm^{-1} and in the opposite direction. This difference in the ν(Cl–F) shift is closely related to the main components of the orbital interactions of each of the structures, discussed previously. As mentioned in the Introduction, the interactions between ClF and several N, O, S, Se, and As- containing compounds, as well as with different alkyne or alkene molecules studied by IR matrix-isolation spectroscopy [6,8–13,16], were previously interpreted as an electron density transfer from the corresponding Lewis base to the lowest unoccupied antibonding molecular orbital of ClF, in accordance with the results presented here.

From the comparison between the experimental and calculated IR spectra described above, it can be concluded that the additional bands in the FTIR spectrum taken immediately after deposition with respect to the FTIR spectra of the monomers, and whose intensities decrease until they disappear after 8 min of irradiation, belong to the $CS_2\cdots ClF$ structure. This is also in agreement with the lower energy predicted for this species. Previous studies on other Lb···ClF complexes (Lb is one of several Lewis bases), either by FTIR matrix-isolation spectroscopy, OCS···ClF [16] and OCSe···ClF [6], or by microwave spectroscopy, $H_2S\cdots ClF$ [14] and $H_2O\cdots ClF$ [14], also conclude that the structures interacting through the chlorine atom of the ClF molecules are the lower-energy forms. Regarding the $CS_2\cdots FCl$ adduct, its presence cannot be completely discarded, since the expected small wavenumber changes would be overlapped to monomer bands. Furthermore, a close inspection of Figure 1 reveals a shoulder of the [ν_{as}(SCS) + ν_s(SCS)] combination

band blueshift by ~2 cm^{-1} that might be tentatively attributed to this complex, taking into account the calculated vibrational data presented in Table 1.

TD-DFT calculations with the B3LYP/6-311+G(d,p) approximation were performed for the optimized $CS_2 \cdots ClF$ structure, to simulate the electronic transitions of this species in the energy range of the irradiation source used for the photochemical experiments, in order to predict the possibility of photolysis of this species under the experimental conditions. The calculated wavelengths for the one-electron transitions are listed in Table 2, together with the theoretical oscillator strength (f) and a tentative approximate assignment. Only transitions with $\lambda > 200$ nm and $f \geq 0.002$ are included in the Table. A schematic representation of the molecular orbitals involved in the electronic transitions presented in Table 2 is presented in Figure 7.

Table 2. Electronic transitions calculated with the TD-DFT (B3LYP/6-311+G(d,p)) approximation for the $CS_2 \cdots ClF$ complex [a].

λ (nm)	Oscillator Strength	Transition	Tentative Approximate Assignment [b]
374.6	0.0002	HOMO → LUMO	π_z (C=S1) → π_z^* (S=C=S)
340.1	0.0010	(HOMO–2) → LUMO	lp_z Cl → π_z^* (S=C=S)
333.9	0.0003	(HOMO–3) → LUMO	π_z (C=S2) → π_z^* (S=C=S)
311.7	0.1381	(HOMO–1) → LUMO	$\pi_{i.p.}$ (C=S1) → π_z^* (S=C=S)
271.7	0.0002	HOMO → (LUM0+2)	π_z (C=S1) → σ* (Cl–F)
263.7	0.2342	(HOMO–1) → (LUM0+2)	$\pi_{i.p.}$ (C=S1) → σ* (Cl–F)
220.7	0.0138	(HOMO–3) → (LUM0+1)	π_z (C=S2) → $\pi_{i.p.}^*$ (S=C=S)
215.2	0.0236	(HOMO–2) → (LUM0+2)	lp_z Cl → σ*(Cl–F)

[a] Only transition with oscillator strength ≥ 0.002 are included. [b] S1 and S2 correspond to the interacting and noninteracting sulfur atom, respectively. The z axis is perpendicular to the molecular plane.

3.2. Photochemistry of CS_2 + ClF in Ar Matrix

The examination of the FTIR spectra taken after irradiation of the matrix allows for the observation that whereas intensities corresponding to the set of bands assigned to the CS_2:ClF molecular complex decrease, another group of bands arises, evidencing the formation of species that were not originally present in the codeposited Ar matrix of CS_2 and ClF at cryogenic temperatures. Some of the IR absorptions appearing after irradiation that could not be associated with any known compound were assigned to novel pentatomic molecules with XC(S)SY general formula, with X, Y = F, Cl, based on (i) the comparison with previous results on similar systems and (ii) the comparison with the IR spectra predicted by DFT methods for these species. Selected spectral regions of the FTIR spectra of the matrix at different irradiation time are presented in Figure 8. A complementary way to evaluate this information is displayed in Figure 9, which shows the variation of band intensities as a function of irradiation time for the signals assigned to the proposed photoproducts.

The region between 1250 and 950 cm^{-1} in the FTIR spectra of the irradiated matrix is particularly rich in information concerning the formation of the new molecules reported in this work. The absorptions at 1228.9/1226.0 and 1213.5/1208.2 cm^{-1}, which grow and then decay on continued irradiation (Figures 8 and 9), were assigned to the ν(C=S) stretching vibration of syn-FC(S)SCl and anti-FC(S)SCl, respectively. The positions of these signals are in very good agreement with the computed wavenumbers at 1220.9 and 1214.0 cm^{-1} using the B3LYP/6-311G+(d,p) level of approximation, as presented in Table 3. According to this computational calculation, the anti-form of FC(S)SCl is the one with the lowest energy. The syn-rotamer is calculated to be 0.76 kcal/mol higher in energy than the anti-form. The IR absorption coefficients values for the ν(C=S) vibrational mode are 383 and 288 km/mol for the syn- and anti-conformer, respectively. Even taking into account the higher absorption coefficient of the syn-rotamer, the experimental abundance of the syn-form is greater than that of the anti-form. Unlike what was observed in other similar photochemical reactions, a process called randomization was not observed in this case [7].

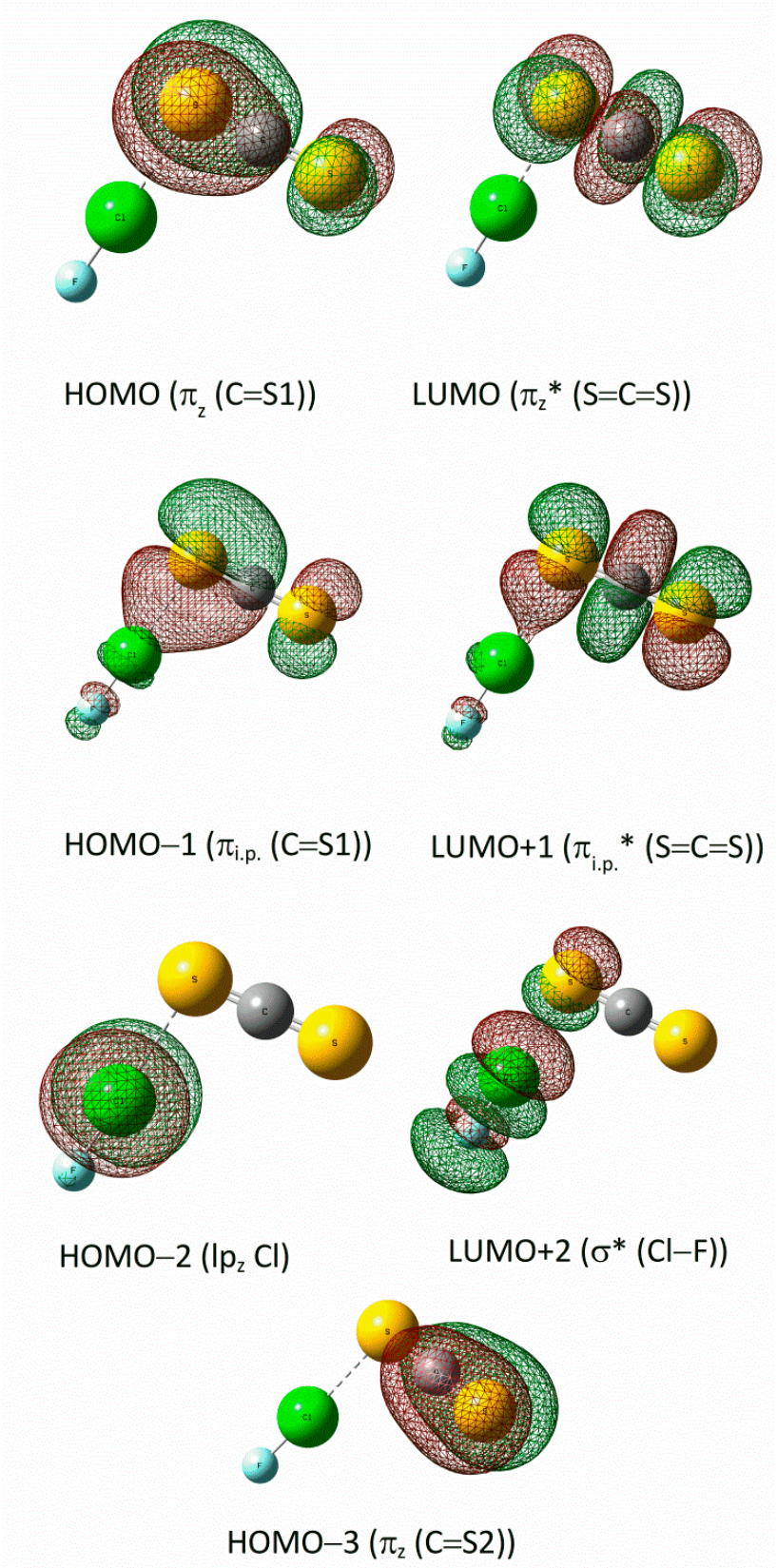

Figure 7. Schematic representation and approximate assignment of the molecular orbitals of the $CS_2\cdots ClF$ complex involved in the electronic transitions with $\lambda > 200$ nm and $f \geq 0.002$, calculated with the B3LYP/6-311+G(d,p) approximation.

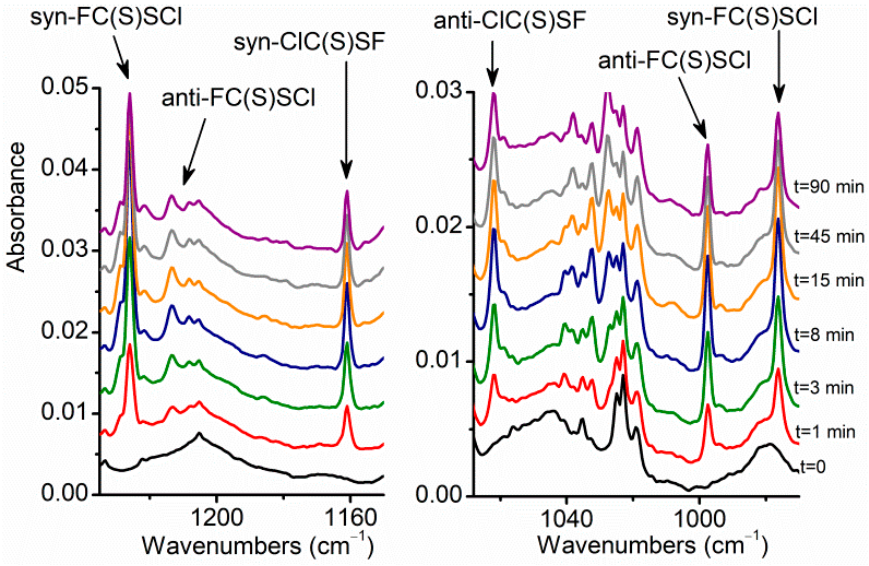

Figure 8. FTIR spectra of the CS_2/ClF/Ar matrix (CS_2:ClF:Ar = 1:2:200) at about 15 K after deposition (**bottom**, black trace) and from **bottom** to **top** after 1 (red trace), 3 (green trace), 8 min (blue trace), 15 min (orange trace), 45 min (grey trace), and 90 min (purple trace) of irradiation with broad-band UV-visible light ($225 \leq \lambda \leq 800$ nm) in the 1235–1150 and 1068–970 cm^{-1} regions.

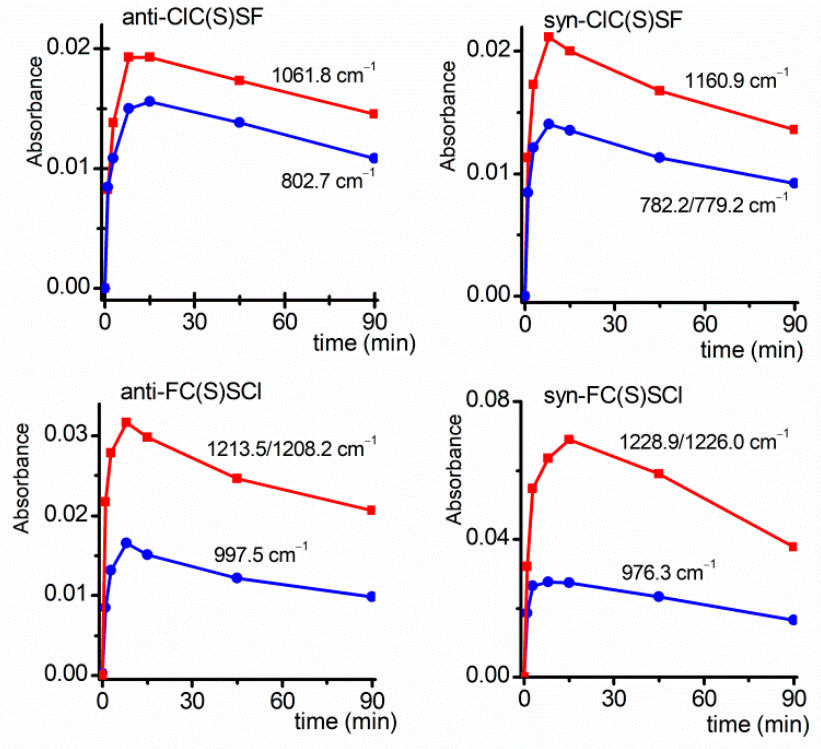

Figure 9. Plots of the intensities of the bands assigned to anti-ClC(S)SF (**top left**), syn-ClC(S)SF (**top right**), anti-FC(S)SCl (**bottom left**) and syn-FC(S)SCl (**bottom right**) in the FTIR spectra of the CS_2/ClF/Ar matrix (CS_2:ClF:Ar = 1:2:200) at about 15 K vs. irradiation times with broad-band UV-visible light ($225 \leq \lambda \leq 800$ nm).

Table 3. Wavenumbers (in cm^{-1}) assigned to syn-FC(S)SCl, anti-FC(S)SCl, syn-ClC(S)SF and anti-ClC(S)SF after irradiation of CS_2/ClF/Ar matrix (CS_2:ClF:Ar = 1:2:200) and computed values with the B3LYP/6-311+G(d,p) approximation (relative IR intensities are given between parentheses).

syn-FC(S)SCl		anti-FC(S)SCl		syn-ClC(S)SF		anti-ClC(S)SF		Tentative
Ar Matrix	Calculated	Ar Matrix	Calculated	Ar Matrix	Calculated	Ar Matrix	Calculated	Assignment
1228.9 1226.0 (100)	1220.9 (100)	1213.5 1208.2 (100)	1214.0 (100)	1160.9 (100)	1159.5 (100)	1061.8 (100)	1084.3 (100)	ν (C=S)
976.3 (40)	965.5 (66)	997.5 (50)	1040.6 (78)	-	743.1 (4)	802.7 (78)	893.6 (56)	ν (C–X) [a]
718.5	589.6 (3)	-	628.9 (2)	-	514.4 (8)	-	481.4 (12)	ν (C–S) [b]
712.2	526.4 (7)	-	464.2 (63)	782.2 779.2 (70)	728.3 (93)	668.8 (50)	671.4 (63)	ν (S–Y)

[a] ν_{as} (Cl–C–S) for syn- and anti-ClC(S)SF. [b] $_{s}$ (Cl–C–S) for syn- and anti-ClC(S)SF.

Two absorptions at 1160.9 and 1061.8 cm^{-1} (Figures 8 and 9) can be attributed to the presence of the bond isomer ClC(S)SF in its two planar syn-ClC(S)SF and anti-ClC(S)SF conformations, respectively. The experimental values compare fairly well with those computed at 1159.5 and 1084.3 cm^{-1} using the B3LYP/6-311G+(d,p) level of approximation (Table 3). The values of the absorption coefficients corresponding to the C=S stretching vibrations of the two rotamers are very similar. According to the performed calculations, the syn-conformer presents an absorption coefficient of 316 km/mol, while a value of 253 km/mol is predicted for the anti-form. The formation kinetics for the two conformers is also similar; the maximum intensity of these absorptions is reached at around 8 min of UV-visible irradiation for both rotamers. As in the case of its FC(S)SCl constitutional isomer, anti-ClC(S)SF was found to be the lowest-energy conformer, being the syn-ClC(S)SF rotamer 2.16 kcal/mol higher in energy than the anti-form. The compared photoevolution of the anti- and syn-ClC(S)SF forms is in this case indicative of a randomization process with approximately equal experimental concentration of each form after irradiation (see Figure S1 in the Supporting Information).

Figure 10 shows the molecular models of the two novel photochemically obtained species, each with its two rotamers, optimized with the B3LYP/6-311+(d,p) approximation. Table S4 of the Supporting Information compiles the theoretical geometric parameters of these species.

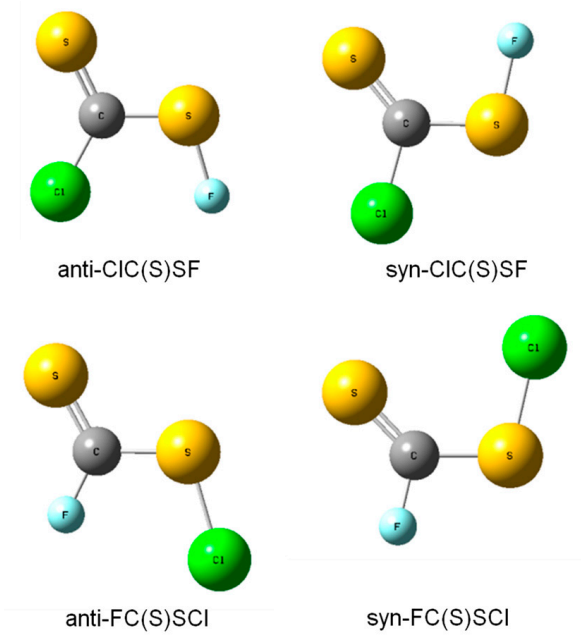

Figure 10. Molecular models of anti-ClC(S)SF, syn-ClC(S)SF, anti-FC(S)SCl and syn-FC(S)SCl calculated with the B3LYP/6-311+G(d,p) approximation.

The presence of anti- and syn-ClC(S)SF rotamers was also reconfirmed experimentally due the additional absorptions appearing when the Ar matrix of codeposited CS_2 and ClF at cryogenic temperatures was irradiated. For the syn-rotamer the computed band at 743.1 cm^{-1} (ν_{as} Cl–C–S) was not observed in the experimental spectra, in accordance with its predicted absorption coefficient of only 9.2 km/mol. The absorption at 782.2/779.2 cm^{-1} could in principle be attributed to the ~778 cm^{-1} IR band of the triatomic species ClSF, isolated by the photolysis of FC(O)SCl in Ar matrix [24]. Although the formation of this molecule cannot be completely discarded, the absence of the other band expected in the recorded region of the spectra, at 543/537 cm^{-1}, allows us to conclude that the major contribution to the signals around 780 cm^{-1} is originated by syn-ClC(S)SF.

In addition to the bands assigned to the XC(S)SY (X, Y = F, Cl) molecules, other features were observed to appear in the IR spectra taken after irradiation. Figure 11 shows the intensity vs. irradiation time plots of the most intense of these IR absorptions. A complete list of the wavenumbers appearing during the irradiation of the CS_2:ClF mixture in Ar matrix, as well as their tentative assignment, is presented in the Supporting Information (Table S5). A weak band at 1481.9 cm^{-1} is developed in the spectra after irradiation. Figure 9 shows the time photoevolution of this absorption, assigned to the ν_{as}(S=C=S) vibrational mode of the Cl•···SCS complex, by the comparison with the reported value at 1481.5 cm^{-1} [5]. Two signals can be observed at 1353.6 and 1346.0 cm^{-1} in the FTIR spectra, attributed to the ν(S=C) vibrational mode of the SCF_2 species [25].

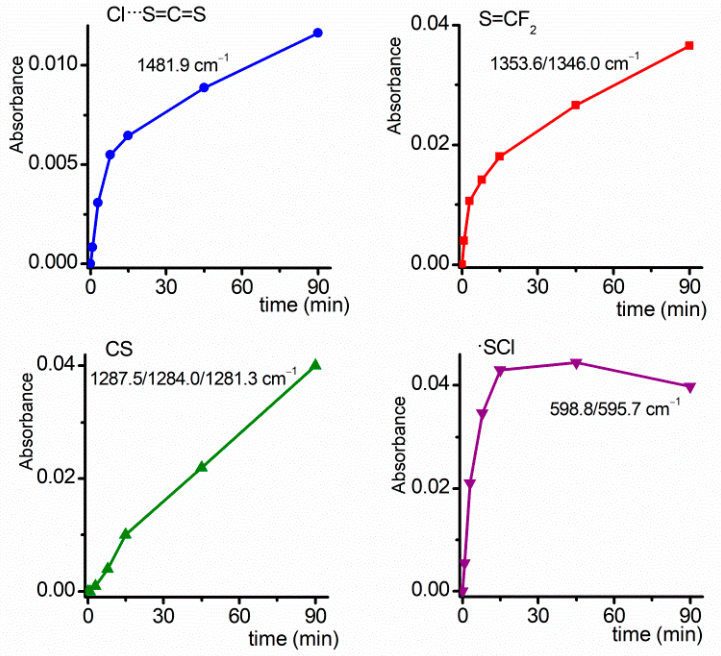

Figure 11. Plots of the intensities of the bands assigned to Cl•···S=C=S (**top left**), $S=CF_2$ (**top right**), CS (**bottom left**) and •SCl (**bottom right**) in the FTIR spectra of the CS_2/ClF/Ar matrix (CS_2:ClF:Ar = 1:2:200) at about 15 K vs. irradiation times with broad-band UV-visible light ($225 \leq \lambda \leq 800$ nm).

A set of bands at 1185.3/1182.2/1179.3 cm^{-1} that follows a similar behavior against the irradiation time and presents the expected intensity ratio with respect to the ν(S=C) mode was attributed to the ν_{as}(F−C−F) of SCF_2, reinforcing the proposed assignment. For its formation, the migration of a F radical from the original matrix cage containing CS_2 and ClF, an already-documented process [26,27], is mandatory. The formation of S=CClF can be ruled out since the most intense FTIR bands of this compound, reported at 1257.4, 1014.9, and 612.4 cm^{-1} [28], are not present in the corresponding vibrational spectra. The absorptions observable at 1287.5, 1284.0, and 1281.3 cm^{-1} can be attributed to complexed CS species, by comparison with its 1276 cm^{-1} reported value for the isolated molecule [29]. A signal with a characteristic $^{35}Cl/^{37}Cl$ pattern, at 598.8/595.7 cm^{-1}, is

tentatively assigned to the SCl• radical, presumably perturbed by the other species present in the same matrix cage (reported values are 574.4 and 566.9 cm^{-1}) [30].

The features observed to develop at 961.5 and 953.2 cm^{-1} (see Figure S2 in the Supporting Information) could not be assigned to any product arising from the CS_2:ClF mixture. Instead, they are originated by the ClClO molecule, formed through the photolysis of Cl_2O [31]. As described in the literature, Cl_2O is a by-product in the preparation of ClF [32]. In fact, the IR absorptions of Cl_2O are present in the initial spectrum of the CS_2:ClF Ar matrix with very low intensities, at 677.1/674.8 and 638.9/636.2/633.5 cm^{-1} [33], and decreased as the bands of ClClO increased.

4. Conclusions

The codeposition of CS_2 and ClF, both diluted in Ar, at about 15 K conducts to the formation of the $CS_2\cdots$ClF complex, as revealed by the comparison of the IR spectrum taken immediately after deposition with the one calculated with DFT methods. Although this complex is predicted to be energetically favorable with respect to the $CS_2\cdots$FCl adduct, the presence of the latter cannot be completely discarded, since if the signals corresponding to this species were present, they would probably be overlapped with those of the monomers due to the expected small wavenumbers shifts. The photolysis of the $CS_2\cdots$ClF species with broad-band UV-visible light ($225 \leq \lambda \leq 800$ nm) is completed after 8 min of irradiation, in agreement with the predicted electronic transitions of this complex by TD-DFT calculations. The first step in the photolysis of the complex isolated in solid Ar is the formation of the constitutional isomers, FC(S)SCl and ClC(S)SF, each of them in their two anti- and syn-rotamers. Although no conclusive evidence exists so far, roaming mechanisms [34] involving either F or Cl atoms could not be ruled out to explain the formation of these two molecules. The novel pentatomic molecules isolated in this work are also photoactive, and evolve inside the Ar-matrix cage, forming CS, the SCl radical, the $CS_2\cdots$Cl complex, and the thiofluorophosgene molecule, F_2CS, in a mechanism that involve the migration of fluorine atoms in the matrix. The proposed photoproducts are summarized in Scheme 1.

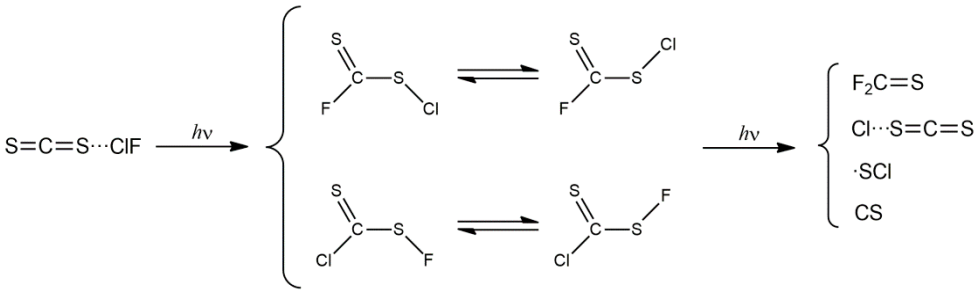

Scheme 1. Proposed photoproducts detected in the FTIR spectra of the CS_2/ClF/Ar matrix (CS_2:ClF:Ar = 1:2:200) at about 15 K after irradiation with broad-band UV-visible light ($225 \leq \lambda \leq 800$ nm).

Supplementary Materials: The following supporting information can be downloaded at: https://www.mdpi.com/article/10.3390/photochem2030049/s1, Figure S1: Plot of the relative intensities of the ν(C=S) absorptions of syn- and anti-ClC(S)SF as a function of the broad-band UV-visible irradiation time; Figure S2: FTIR spectra of the CS_2/ClF/Ar matrix (CS_2:ClF:Ar = 1:2:200) at about 15 K after deposition (bottom, black trace) and (from bottom to top) 1 (red trace), 3 (green trace), 8 min (blue trace), 15 min (orange trace), 45 min (grey trace) and 90 min (purple trace) of irradiation with broad-band UV-visible light ($225 \leq \lambda \leq 800$ nm) in the 970–940 and 655–635 cm^{-1} regions; Figure S3: Plot of the relative intensities of the ν(C=S) absorptions of syn- and anti-ClC(S)SF as a function of the broad-band UV-visible irradiation time; Figure S4: FTIR spectra of the CS_2/ClF/Ar matrix (CS_2:ClF:Ar = 1:2:200) at about 15 K after deposition (bottom, black trace) and (from bottom to top) 1 (red trace), 3 (green trace), 8 min (blue trace), 15 min (orange trace), 45 min (grey trace) and 90 min (purple trace) of irradiation with broad-band UV-visible light ($225 \leq \lambda \leq 800$ nm) in the 970–940 and 655–635 cm^{-1} regions; Table S1: Geometric parameters for the different complexes formed between CS_2 and ClF (distances in Å, angles in degrees) calculated using the B3LYP/6-

311+G(d,p) approximation; Table S2: $\Delta E^{(SCF)}$, ΔE^{CP}, BSSE and GEOM corrections (in kcal.mol^{-1}), transferred charge (q), orbital stabilization energy ($\Delta E^{(2)}$ in kcal.mol^{-1}) for the different complexes formed between CS_2 and ClF computed using the B3LYP/6-311+G(d,p) approximation; Table S3: Wavenumbers for the different complexes formed between CS_2 and ClF computed with the B3LYP/6-311+G(d,p) approximation (wavenumbers are in cm^{-1} and relative IR intensities are given between parentheses) and comparison with the experimental values; Table S4: Geometrical parameters of anti-ClC(S)SF, syn-ClC(S)SF, anti-FC(S)SCl, and syn-FC(S)SCl calculated with the B3LYP/6-311+G(d,p) approximation (distances in Å and angles in degrees); Table S5: FTIR wavenumber and proposed assignment of the photoproducts formed by UV-visible irradiation of CS_2 and ClF co-deposited in an Ar matrix (CS_2:ClF:Ar 1:2:200) at cryogenic temperatures. Refs. [5,25,29,30,35] have been cited in supplementary materials.

Author Contributions: Conceptualization, C.O.D.V. and R.M.R.; formal analysis, M.T.C.C., C.O.D.V. and R.M.R.; investigation, C.O.D.V. and H.W.; writing—original draft preparation, C.O.D.V. and R.M.R.; writing—review and editing, C.O.D.V. and R.M.R.; funding acquisition, C.O.D.V. and R.M.R. All authors have read and agreed to the published version of the manuscript.

Funding: This research was funded by Consejo Nacional de Investigaciones Científicas y Técnicas (CONICET), PIP 0352, Agencia Nacional de Promoción Científica y Tecnológica (ANPCyT), PICT-2014-3266 and PICT-2018-04355, Universidad Nacional de La Plata, UNLP-X822.

Institutional Review Board Statement: Not applicable.

Informed Consent Statement: Not applicable.

Data Availability Statement: Not applicable.

Conflicts of Interest: The authors declare no conflict of interest.

References

1. Ault, B.S. Matrix isolation spectroscopic studies: Thermal and soft photochemical bimolecular reactions. *Front. Adv. Mol. Spectrosc.* **2018**, *20*, 667–712.
2. Wu, Z.; Shao, X.; Zhu, B.; Wang, L.; Lu, B.; Trabelsi, T.; Francisco, J.S.; Zeng, X. Spectroscopic characterization of two peroxyl radicals during the O_2-oxidation of the methylthio radical. *Commun. Chem.* **2022**, *5*, 19. [CrossRef]
3. Young, N.A. Main group coordination chemistry at low temperatures: A review of matrix isolated Group 12 to Group 18 complexes. *Coord. Chem. Rev.* **2013**, *257*, 956–1010. [CrossRef]
4. Bava, Y.B.; Cozzarín, M.V.; Della Védova, C.O.; Willner, H.; Romano, R.M. Preparation of FC(S)SF, FC(S)SeF and FC(Se)SeF through matrix photochemical reactions of F_2 with CS_2, SCSe, and CSe_2. *Phys. Chem. Chem. Phys.* **2021**, *23*, 20892–20900. [CrossRef]
5. Tobón, Y.A.; Romano, R.M.; Della Védova, C.O.; Downs, A.J. Formation of new halogenotiocarbonylsulfenyl halides, XC(S)SY, through photochemical matrix reactions starting from CS_2 and dihalogen molecule XY (XY = Cl_2, Br_2, or BrCl). *Inorg. Chem.* **2007**, *46*, 4692–4703. [CrossRef]
6. Gomez Castaño, J.A.; Romano, R.M.; Della Védova, C.O.; Willner, H. Photochemical reaction of OCSe with ClF in argon matrix: A light-driven formation of XC(O)SeY (X, Y = F or Cl) species. *J. Phys. Chem. A* **2017**, *121*, 2878–2887. [CrossRef]
7. Gómez Castaño, J.A.; Picone, A.L.; Romano, R.M.; Willner, H.; Della Védova, C.O. Early barriers in the matrix photochemical formation of syn–anti randomized FC(O)SeF from the OCSe:F_2 complex. *Chem. Eur. J.* **2007**, *13*, 9355–9361. [CrossRef]
8. Ault, B.S. Matrix isolation investigation of the interaction of CIF and Cl_2 with carbon-carbon multiple bonds. *J. Phys. Chem.* **1987**, *91*, 4723–4727. [CrossRef]
9. Machara, N.P.; Ault, B.S. Infrared spectroscopy studies of the interactions of CIF and Cl_2 with H_2Se, $(CH_3)_2Se$ and AsH_3 in argon matrices. *Inorg. Chem.* **1988**, *27*, 2383–2385. [CrossRef]
10. Bai, H.; Ault, B.S. Infrared spectroscopy investigation of complexes of CIF and Cl_2 with crown ethers and related cyclic polyethers in argon matrices. *J. Mol. Struct.* **1989**, *196*, 47–56. [CrossRef]
11. Bai, H.; Ault, B.S. Infrared matrix isolation of the 1 1 complexes of HCl and CIF with sulfur and nitrogen-containing macrocycles. *J. Mol. Struct.* **1990**, *238*, 223–230. [CrossRef]
12. Bai, H.; Ault, B.S. Infrared matrix isolation investigation of the molecular complexes of CIF with benzene and its derivatives. *J. Phys. Chem.* **1990**, *94*, 199–203. [CrossRef]
13. Bai, H.; Ault, B.S. Matrix isolation study of complexation and with terf-butyl halides. *J. Phys. Chem.* **1991**, *95*, 3080–3084. [CrossRef]
14. Bloemink, H.I.; Hinds, K.; Holloway, J.H.; Legon, A.C. Isolation of H_2S...C1F in a pre-reactive mixture of H_2S and C1F expanded in a coaxial jet and characterisation by rotational spectroscopy. *Chem. Phys. Lett.* **1995**, *242*, 113–120. [CrossRef]

15. Cooke, S.A.; Cotti, G.; Evans, C.M.; Holloway, J.H.; Kisiel, Z.; Legon, A.C.; Thumwood, J.M.A. Pre-reactive complexes in mixtures of water vapour with halogens: Characterisation of $H_2O\cdots ClF$ and $H_2O\cdots F_2$ by a combination of rotational spectroscopy and ab initio calculations. *Chem. Eur. J.* **2001**, *7*, 2295–2305. [CrossRef]
16. Picone, A.L.; Della Védova, C.O.; Willner, H.; Downs, A.J.; Romano, R.M. Experimental and theoretical characterization of molecular complexes formed between OCS and XY molecules (X, Y = F, Cl and Br) and their role in photochemical matrix reactions. *Phys. Chem. Chem. Phys.* **2010**, *12*, 563–571. [CrossRef]
17. Schnöckel, H.; Willner, H. Matrix-isolated molecules. In *Infrared and Raman Spectroscopy, Methods and Applications*; Schrader, B., Ed.; VCH: Weinheim, Germany, 1995; pp. 297–313.
18. Frisch, M.J.; Trucks, G.W.; Schlegel, H.B.; Scuseria, G.E.; Robb, M.A.; Cheeseman, J.R.; Montgomery, J.A., Jr.; Vreven, T.; Kudin, K.N.; Burant, J.C.; et al. *Gaussian 03, Rev. B.04*; Gaussian, Inc.: Pittsburgh, PA, USA, 2003.
19. Frisch, M.J.; Trucks, G.W.; Schlegel, H.B.; Scuseria, G.E.; Robb, M.A.; Cheeseman, J.R.; Scalmani, G.; Barone, V.; Mennucci, B.; Petersson, G.A.; et al. *Gaussian 09, Rev. D.01*; Gaussian, Inc.: Wallingford, CT, USA, 2013.
20. Nagy, P.I.; Smith, D.A.; Alagona, G.; Ghio, C. Ab initio studies of free and monohydrated carboxylic acids in the gas phase. *J. Phys. Chem.* **1994**, *98*, 486–493. [CrossRef]
21. Boys, S.F.; Bernardi, F. The calculation of small molecular interactions by the differences of separate total energies. Some procedures with reduced errors. *Mol. Phys.* **1970**, *19*, 553–566. [CrossRef]
22. Bauernschmitt, R.; Ahlrichs, R. Treatment of electronic excitations within the adiabatic approximation of time dependent density functional theory. *Chem. Phys. Lett.* **1996**, *256*, 454–464. [CrossRef]
23. Stratmann, R.E.; Scuseria, G.E.; Frisch, M.J. An efficient implementation of time-dependent density-functional theory for the calculation of excitation energies of large molecules. *J. Chem. Phys.* **1998**, *109*, 8218–8224. [CrossRef]
24. Willner, H. Das Infrarotspektrum von matrixisoliertem SFCl. *Z. Für Nat. B* **1984**, *39*, 314–316. [CrossRef]
25. Haas, A.; Willner, H.; Bürger, H.; Pawelke, G. Matrix-infrarot-Spektren und Kraftkonstanten von SCF_2 und $SeCF_2$. *Spectrochim. Acta* **1977**, *33*, 937–945. [CrossRef]
26. Alimi, R.; Gerber, R.B.; Apkarian, V.A. Dynamics of molecular reactions in solids: Photodissociation of F_2 in crystalline Ar. *J. Chem. Phys.* **1990**, *92*, 3551–3558. [CrossRef]
27. Feld, J.; Kunttu, H.; Apkarian, V.A. Photodissociation of F_2 and mobility of F atoms in crystalline argon. *J. Chem. Phys.* **1990**, *93*, 1009–1020. [CrossRef]
28. Hamm, R. Schwingungsspektrum von CSFCl. *Z. Naturforsch.* **1979**, *34 A*, 325–332. [CrossRef]
29. Jacox, M.E.; Milligan, D.E. Matrix isolation study of the infrared spectrum of thioformaldehyde. *J. Mol. Spectrosc.* **1975**, *58*, 142–157. [CrossRef]
30. Willner, H. Die Infrarotabsorption des matrixisolierten SCl-Radikal. *Spectrochim. Acta* **1981**, *37*, 405–406. [CrossRef]
31. Johnsson, K.; Engdahl, A.; Nelander, B. The UV and IR Spectra of the ClClO Molecule. *J. Phys. Chem.* **1995**, *99*, 3965–3968. [CrossRef]
32. Ruff, O.; Ascher, E.; Lass, F. Das Chlorfluorid. *Z. Anorg. Allg. Chem.* **1928**, *176*, 258–270. [CrossRef]
33. Andrews, L.; Raymond, J.I. Argon matrix infrared spectrum of the ClO radical. *J. Chem. Phys.* **1971**, *55*, 3087–3094. [CrossRef]
34. Townsend, D.; Lahankar, S.A.; Lee, S.K.; Chambreau, S.D.; Suits, A.G.; Zhang, X.; Rheinecker, J.; Harding, L.B.; Bowman, J.M. The roaming atom: Straying from the reaction path in formaldehyde decomposition. *Science* **2004**, *306*, 1158–1161. [CrossRef] [PubMed]
35. Bondi, A. van der Waals Volumes and Radii. *J. Phys. Chem.* **1964**, *68*, 441–451.